Proc. (CD), 12th Intern. Conf. on Fracture (ICF-12) (held in Ottawa, Canada, July 2009), Robert Bell, ed., Carleton University, pp. 1–10.

Size Effect on Strength of Bimaterial Joints: Computational Approach versus Analysis and Experiment

Jia-Liang Le[1], Ferhun C. Caner[2], Qiang Yu[1], and Zdeněk P. Bažant[1]
[1]*Northwestern University, IL, USA;* [2]*Technical University of Catalonia, Spain*

Abstract

Metal-composite joints connecting conventional steel to an advanced fiber composite are an attractive structural system for hybrid ship hulls as well as aircraft frames. The objective of this study is to analyze the size effect on the strength of hybrid joints numerically, theoretically and experimentally. In the numerical analysis, linear elastic continuum elements are used for the composite and steel while cohesive fracturing zero-thickness elements are used for the steel-composite interface. The numerically simulated size effect on the strength of the joints is verified by analytical and experimental studies. Analytical formulation of the asymptote of size effect law is anchored at the large size limit by LEFM (linear elastic fracture mechanics) solutions with complex singularity. A general approximate size effect law, spanning all sizes, is further derived via asymptotic matching. The experimental studies involve testing of geometrically similar specimens with size ratio of 1:4:12. The analytical, numerical and experimental studies all indicate that the strength of metal-composite joints exhibits a strong size effect.

1. Introduction

Bimaterial joints of metal and fiber composite, with a very thin adhesive between them, are the crucial component of an effective structural system for large ships [1]. They are also needed for large fuel-efficient aircraft. Due to the stress concentration caused by the corner geometry and material mismatch, the bimaterial corners are the critical locations for the design of hybrid joints. Fracture mechanics of various bimaterial joints has been extensively investigated [2, 3]. However, the scaling of fracture and associated size effect for such joints have not yet been explored. Previous studies have shown that fiber composite structures exhibit a strong size effect [4-7], and so one may expect the same to occur in the hybrid joints as well. Correct understanding of the size effect on the strength of joints is important for correct extrapolation of small-scale laboratory test results to full-size joints.

In this study, we consider a double-lap hybrid joint specimen shown in Fig. 1a. We define the nominal strength $\sigma_N = P_{max}/bD$, where P_{max} = maximum load, b = width of the specimen (in the third dimension), and D = in-plane characteristic dimension. Here we chose D = interface length (Fig. 1a). To avoid small secondary effects of the length of crack front edge in the third dimension (stemming from a transition from plane strain to plane stress along the edge), it is better to consider two-dimensional similarity, i.e., set the width b = constant. This paper aims to study numerically, analytically and experimentally the effect of structure size D on the nominal strength σ_N of the hybrid joint.

2. Computational Simulation of Metal-Composite Joints

Computational simulation of the metal-composite joints plays an important role in this study, not only to obtain the size effect law for small size structures, but also to design the specimen dimensions for experimental studies. For accurate determination of the size effect on the strength of joints, the experimental investigations should span a large size range. Thus large variations of the skin thickness are required.

In this study, we are interested in interfacial failure; hence all the specimens must be designed to fail in this manner. Therefore, it is important to determine the maximum load below which the skin and steel block thicknesses would suffice to avoid axial tensile failure of the skins as well as plastic yielding of the steel block. This maximum load depends not only on the shear strength of the interface, but also on the fracture energy.

It is well known that, for the purposes of size effect calculations (i.e. calculation of peak loads), only the initial tangent of the cohesive law is relevant. Thus, the cohesive law assumed in the calculations is a linear softening law governing the fracture of the steel-composite interface, as shown in Fig. 2. In the finite element model, the steel block of the hybrid joint is discretized by hexahedral finite elements with an isotropic linear elastic material law. For the continuum element that discretizes the composite skin, orthotropic linear elasticity is assumed. At the steel-composite interface, cohesive fracturing zero-thickness interface elements made up of two four-node quadrilaterals, which connect the faces of two adjacent hexahedral continuum elements, are inserted. In these elements, the surfaces of the two quadrilaterals are initially coincident. During the loading, these surfaces are allowed to separate or slip, to simulate crack opening or shearing fracture, and their relative normal and shear displacements produce normal and shear stresses, captured at Gauss points of these finite elements according to the prescribed constitutive law. The detailed FEM formulation and its implementation can be found in [8].

The simulations for mesh size sensitivity of the failure load of specimens of all sizes were performed first. It was suspected that when the LEFM limit is approached for large sizes, the finite element model had to employ a fine mesh at the fracturing interface; otherwise the cohesive fracturing interface elements would not have been able to capture the nearly singular stress field at the crack front. It has been found that, indeed, using a different number of elements in the fracturing interface gave rise to different “simulated” scaling of failure stress with size. For example, when all interfaces were discretized using only 10 zero-thickness interface elements along the interface length for all sizes, there was no size effect, i.e., the failure happened always at the same nominal stress for all the sizes, implying that the “simulated” scaling of strength with size had a zero exponent. But when the number of elements was increased to more than 150, it was found that the “simulated” strength scaled with a size exponent of approximately −0.5, which is very close to the LEFM scaling for the design size range. This is a demonstration of the fact that, to obtain accurate finite element predictions of the peak loads of structures failing by quasi-brittle fracture, it is necessary to have knowledge about the scaling of strength with size, or else mesh sensitivity analyses need to be performed before the finite element results could be trusted.

The “simulated” size effect curve obtained from the finite element calculations is shown in Fig. 3. For the practical size range of hybrid joints, there does not seem to be a significant transition from the LEFM scaling law for large sizes toward the strength based scaling with a vanishing size exponent for small sizes. Note that the computational model described here can be conveniently used for determining the cohesive fracture parameters from experiments. This can be done by calibrating the model to simultaneously fit the experimental results for all the sizes.

3. Analytical Formulation of the Asymptotics of Size Effect Law

The asymptotic properties of the size effect law for large sizes can be analytically obtained from the linear elastic fracture mechanics. Since both the loading and the geometry of the specimen are symmetric, the elastic field must be symmetric before the peak load is attained. Therefore, we analyze only one quarter of the specimen (Fig. 1b). In this quarter, there are two critical bimaterial corners where the corner geometry and material mismatch cause singularity and stress concentration. To identify the critical corner from which the crack propagates, the stress singularity exponents must be calculated.

In this study, a complex field method is used to calculate the displacement singularity [9]. Under plane loading conditions, the elastic field (displacement, traction, and stress fields) in the material can be represented by two holomorphic functions $f_1(z_1)$ and $f_2(z_2)$ where $z_i = x + \mu_i y$; μ_i is the root with positive imaginary part of the 4th order equation $\lambda\mu^4+2\rho\lambda^{0.5}\mu^2+1 = 0$ where $\lambda = s_{11}/s_{22}$ and $\rho = 0.5(2s_{12}+s_{66})(s_{11}s_{22})^{-1/2}$ (s_{ij} = element of general material compliance matrix). For the near-corner elastic field, these two holomorphic functions can be written as: $f_k(z_k) = \phi_k r^{\delta}(\cos\theta + \mu_k \sin\theta)^{\delta}$ $(k = 1, 2)$, where δ = displacement singularity exponent. By imposing the traction and displacement at two exterior boundaries and the interface, one obtains a system of linear equations, which can be written in a matrix form $K(\delta)\nu = 0$. The displacement singularity δ can be obtained by setting Det(K) = 0. To obtain it numerically, we choose here to seek the value of δ for which the condition number of matrix K becomes very large.

According to the experimental investigations which will be reported in the subsequent section, the orthotropic elastic constants of the fiber composite used in this study are: E_1 = 21 GPa, E_2 =9.5 GPa, ν_{12} = 0.2, G_{12} = 3.0 GPa. For steel, which is isotropic, E = 200 GPa, ν = 0.3. Fig. 4 shows the plot of Det(K) in the complex plane of the displacement singularity. At the left corner of the joint (at which the stiffer material terminates), the displacement field is found to exhibit singularities with exponents representing a pair of complex conjugates : δ = 0.537 $\pm$ 0.07i and, at the right corner (at which the softer material terminates) a real displacement singularity δ = 0.78. So, the singularity at the left corner is much stronger than it is at the right corner. Hence, the crack is expected to start propagating from the left corner, which agrees with experimental observations. This is the corner that governs the strength of the hybrid joint, and so the fracture needs to be investigated only for that corner.

Various fracture criteria have been proposed to characterize the crack initiation for general bimaterial corners [10, 11]. Due to the nature of mix-mode fratcure at bimaterial corner, the use of stress intensity factors as a fracture criterion necessitates an empirical equation involving modes I and II stress intensity factors. A more general and effective approach is to consider the energy release rate or the corresponding fracture toughness as the failure criterion.

Consider a bimaterial corner with the strongest stress singularity $\lambda = \kappa \pm i\eta$. The near-tip stress field can be written as

$$\sigma_{ij} = \mathrm{Re}[Hr^{i\eta} f_{ij}(\theta,\eta)]r^{\kappa} \tag{1}$$

where H is the stress intensity factor, which is in general complex. Dimensional analysis shows that H must have the form:

$$H = \frac{P}{bD} D^{-\kappa} \left|h(\eta,\varphi)\right| e^{i(\omega-\eta \ln D)} \tag{2}$$

where P = applied load, b = width of the joint, D = characteristic size of the joint (= interface length), $h(\eta,\varphi)$ = dimensionless complex stress intensity factor, φ = effective loading angle (which combines the effects of loading angle and boundary conditions), and ω = phase angle of $h(\eta,\varphi)$.

Once the crack initiates from the corner tip, it will propagate along the path that corresponds to the highest energy dissipation by fracture. The adhesive layer, which connects the fiber composite and the steel and is as thin as possible, is normally in hybrid joints designs much weaker than both materials, and so the crack is expected to propagate along the interface.

The initiation of a crack, or macro-crack, requires formation of a microcracking zone of a certain finite characteristic length l_{FPZ} within (and possibly near) the adhesive layer. This zone, called the fracture process zone (FPZ) develops stably and transmits cohesive stresses. As soon as the full FPZ develops, the maximum load is attained. After that, the equilibrium load will be assumed to decrease, which requires the geometry to be positive [12] (this is normally satisfied but, of course, needs to be verified).

In analogy to the derivation of the size effect law for cracks in homogenous solids [13], we may assume that, not too close to the FPZ, the effect of a finite-size FPZ on the elastic field is approximately equivalent to the effect of an interface crack of a certain finite effective length c_f (which is proportional to the length of the FPZ, l_{FPZ}, and is cca $l_{FPZ}/2$) [12, 13]. Therefore, what matters at the maximum load in a large enough joint is the asymptotic field near of the interface crack, rather than of a corner.

In the foregoing, a distinction is made between: 1) the near-tip asymptotic field of the imagined effective crack substituted for the overall effect of the FPZ; 2) the near-tip field of the corner applied not too close to the tip of the crack so that it can envelop the near-tip field of the crack; and 3) the far-away field affected by the boundary conditions. These fields are here matched energetically, through the strength of the singularities. Note that the second field corresponds to what has been conceived by Barenblatt [14] as the intermediate asymptotic. The intermediate asymptotic is relevant if $D >> D' >> l_{FPZ}$ (D' = the size of the corner tip singular field), and the near tip field of a crack is applicable only if the radial distance from crack tip $r << l_{FPZ}$, i.e. in the large-size limit.

In the large-size asymptotic limit, the asymptotic near-tip field of the hypothetical interface crack of length c_f, substituted for the FPZ, must be surrounded by the singular stress field of a bimaterial corner tip (except when the laminate thickness is too small, which has been checked not to be the case in practical situations). Therefore, the stress intensity factor K at the interfacial crack tip will depend on the stress field whose magnitude is characterized by the stress intensity factor H of the corner tip. By dimensional analysis, the two stress intensity factors may be related as [10, 15]:

$$Kc_f^{\,i\eta'} = Hc_f^{\,\kappa+0.5}c_f^{\,i\eta} f \tag{3}$$

where f = dimensionless complex number. For the interfacial crack, it is well known that the energy release rate function for an interfacial crack can always be written as [16]:

$$\mathcal{G} = \frac{CK\overline{K}}{E} \tag{4}$$

Upon substituting Eqs. 2 and 3 into the foregoing equation, one obtains:

$$\mathcal{G} = \frac{\sigma^2 D^{-2\kappa}}{Ec_f^{\,-1-2\kappa}}|g|^2 \tag{5}$$

where σ = nominal stress = P/bD, and $|g|$ = C $|f|$ $|h|$. Within the LEFM framework, a crack can propagate once $\mathcal{G}$ reaches a certain critical value G_f, called the fracture energy, and this also represents the condition of maximum load

P. From Eq. 5, one obtains the LEFM expression of nominal strength σ_N (= P/bD) of the bimaterial joint:

$$\sigma_N = |g|^{-1}\sqrt{EG_f}\, c_f^{\,-\kappa-0.5} D^{\kappa} \tag{6}$$

Eq. 6 represents the large-size asymptote of the size effect law. It is clear that this asymptote follows a power scaling law, with an exponent directly related to the real part of the strongest stress singularity exponent for the bimaterial corner tip.

A general approximate formula for the size effect on the nominal strength σ_N, spanning all the sizes and a range of corner angles, can be obtained through asymptotic matching [13]. A general approximate size effect equation has recently been developed for symmetrically loaded reentrant corners in homogenous materials of various corner angles, which exhibit a real singularity [17]. For the general case with complex singularity, the aforementioned analysis shows that only the real part of singularity exponent matters for the energy release rate. Therefore, an equation of similar type can be used to approximate the general size effect law for the hybrid joint :

$$\sigma_N = \sigma_0 \left(1 + \frac{D}{D_{0\beta}}\right)^{\kappa(\beta)} \tag{7}$$

where σ_0 and $D_{0\beta}$ are parameters yet to be calibrated by the size effect tests, κ = real part of the strongest stress singularity exponent at the bimaterial corner, which is a function of corner angle β. Note that the foregoing equation has been set up to match three essential asymptotic conditions:

1) For $D/l_0 \to 0$, there must be no size effect since the FPZ occupies the whole structure and what matters is solely the material strength, and not the energy release (the failure is quasi-plastic).

2) For $D/l_0 \to \infty$, Eq. 7 must match Eq. 6 as the large-size asymptote of size effect law.

3) For $\beta = \pi$ (smooth surface, no corner), the size effect of this type must vanish (there is another type of size effect (Type 1), applicable to failures at cohesive crack initiation from a smooth surface).

4. Experimental Investigation on Size Effect Law

Based on preliminary computer simulations, 9 specimens were designed and manufactured, see Fig. 5a. To ensure that the axial tensile force is applied through the center line of the specimen, the specimen is connected to the loading piston through a steel chain at each end (Fig. 5b). Except for the end portion connected by a steel pin, the specimens are geometrically similar, with the scaling ratio 1:4:12. The composite material used in this study is fiberglass-epoxy laminates (G-10/FR4 Epoxy Grade procured from McMaster-Carr, Inc.). The uniaxial tension, compression, and Iosipescu V-notch beam shear tests are conducted to obtain the elastic constants of the composite. The adhesive used to glue the laminate to the steel block is E-60 HP metal-plastic bonder with high shear strength and high peel resistance.

The specimens are loaded under displacement control by an MTS machine. To eliminate differences due to the rate effect, it is essential to ensure that, for all the specimens, the FPZ is fully formed within approximately the same time duration. In all the tests, the maximum load was reached in about 5 to 6 minutes. It is observed that all the specimens failed by interfacial fracture. By careful investigation of the damage pattern, one finds the damage of the laminate to be concentrated in the regions near the interior corners of the joint. Therefore, the crack in the interface must have initiated from the inner corner, as predicted by both the computational and analytical studies.

A strong size effect can be seen in the plot of the nominal strength σ_N versus the specimen size D. By least-square statistical regression, one can calibrate the analytical size effect expression derived in the preceding, as shown in Fig. 6. Note that the asymptotic slope of the theoretical size effect curve agrees well with the test data.

5. Conclusion

The analytical study indicates that the large size asymptote of size effect law follows a power law with an exponent related to the order of the stress singularity. The generalized size effect law, which is developed through asymptotic matching, is shown to fit the experimental results very well. The numerical, analytical and experimental studies all show a strong size effect on the strength of the hybrid joint.

Acknowledgement

Financial support under Grant N00014-07-0313 from the Office of Naval Research, monitored by Dr. Roshdy Barsoum, is gratefully acknowledged.

References:

[1] Barsoum, R.S., “The best of both worlds : Hybrid ship hulls use composite & steel.” The AMPTIAC Quarterly 7 (3), 55-61.

[2] Bahei-El-Din, Y.A. and Dvorak, G.J. “New designs of adhensive joints for thick composite laminates.” Composites Sci. and Tech. 61, 2001, 19-40.

[3] Dvorak, G.J., Zhang, J., and Canyurt, O. “Adhesive tongue-and-groove joints for thick composite laminates.” Composites Sci. and Tech. 61, 2001, 1123-1142.

[4] Bažant, Z.P., Zhou, Y., Daniel, I.M., Caner, F.C., and Yu, Q. "Size effect on strength of laminate-foam sandwich plates." J. Eng. Mater. Tech. ASME 128 (3), 2006, 366-374.

[5] Bažant, Z.P., Zhou, Y., Novak, D., and Daniel, I.M. "Size effect on flexural strength of fiber-composite laminate." ASME J. Eng. Mater. Tech. 126, 2004, 29-37.

[6] Bažant, Z.P., Daniel, I.M., and Li, Z. "Size effect and fracture characteristics of composite laminates." J. Eng. Mater. Tech. ASME 118 (3), 1996, 317-324.

[7] Bažant, Z.P., Kim, J.-J.H. Kim, Daniel, I.M., Becq-Giraudon, E., and Zi, G. "Size effect on compression strength of fiber composites failing by kink band propagation." Int. J. Fract. 95, 1999, 103-141.

[8] Caner, F.C. and Bažant Z.P. "Size effect on strength of laminate-foam sandwich plates: Finite element analysis with interface fracture", Int. J. of Solids and Structures. 2007, (submitted)

[9] Desmorat, R. and Leckie, F.A. "Singularities in bi-materials: parametric study of an isotropic/anisotropic joint." Eur. J. Mech., A/Solids 17, 1998, 33-52.

[10] Grenestedt, J.L. and Hallstrom, S. "Crack initiation from homogeneous and bi-material corners." J. Appl. Mech. ASME 64 (December), 1997, 811-818.

[11] Leguillon, D. "Strength or toughness? A criterion for crack onset at a notch." Eur. J. Mech., A/Solids 21, 2002, 61-72.

[12] Bažant, Z.P. and Planas, J. Fracture and Size Effect in Concrete and Other Quasibrittle Materials, CRC Press, 1997.

[13] Bažant, Z.P. Scaling of Structural Strength. Hermes Penton Science, London; 2nd updated ed., Elsevier 2005.

[14] Barenblatt, G.I. Scaling, Self-Similarity and Intermediate Asymptotics. Cambridge University Press, Cambridge, UK, 1996.

[15] Liu, D. and Fleck, N.A. "Scale effect in the initiation of cracking of a scarf joint." Int. J. Fract. 95, 1999, 66-88.

[16] Hutchinson, J.W. and Suo, Z. "Mixed mode cracking in layered materials." Adv. Appl. Mech. 29, 1992, 64-191.

[17] Bažant, Z.P. and Yu, Q. "Size effect on strength of quasibrittle structures with reentrant corners symmetrically loaded in tension." J. Eng. Mech. ASCE 129 (11), 2006, 1168--1176.

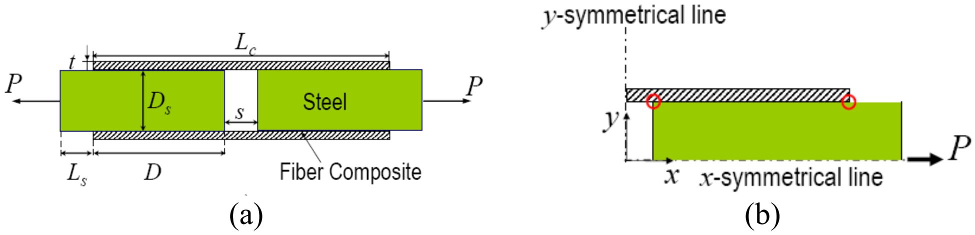

Figure 1. Geometry of double-lap hybrid joint

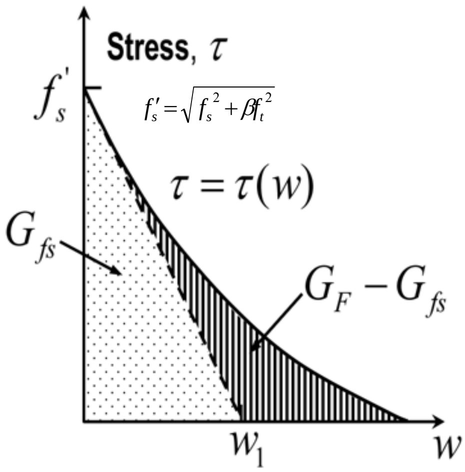

Figure 2. Cohesive law for interfacial fratcure

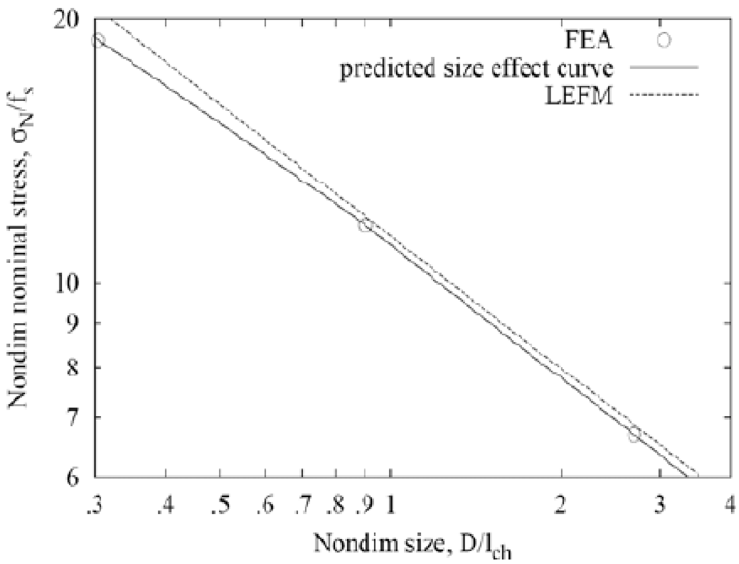

Figure 3. Similated size effect curve

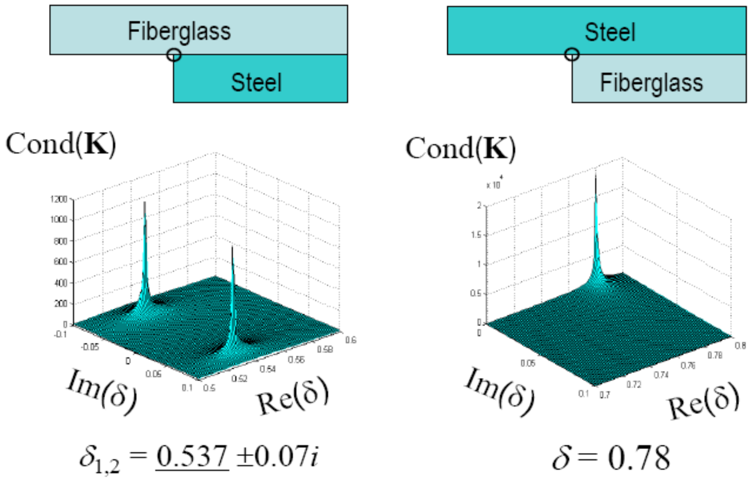

* Cond = condition number of the matrix

Figure 4. Exponent of displacement singularity

a) b)

Figure 5 a) test specimens; b) test set-up

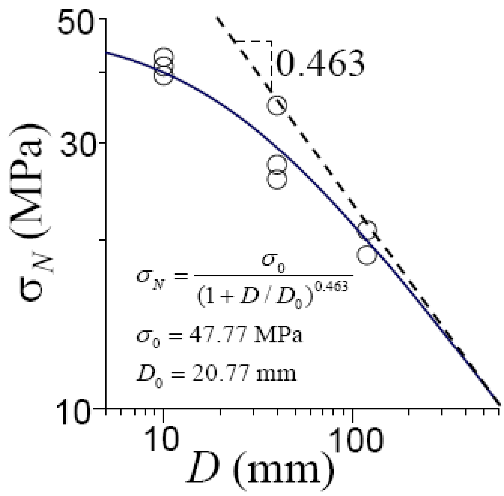

Figure 6 Calibration of size effect law